INTERNATIONAL JOURNAL OF GEOMAGNETISM AND AERONOMY
VOL. 3, NO. 3, PAGES 255–260, FEBRUARY 2003

A storm in the magnetospheric magnetic field

Yu. P. Maltsev and A. A. Ostapenko

Polar Geophysical Institute, Apatity, Russia

Abstract. Several tens of hundreds of magnetic field measurements were used to study the statistical field behavior at distances of up to $30R_E$ for different levels of the Dst index. It has been found that in the major part of the magnetospheric equatorial plane a magnetic field depression which increases during a storm takes place. The point where the depression is maximal is located at night at the distance of several R_E. The field in the tail lobes grows as the storm enhances, the maximum increase occurring in the tail lobes nearest to the Earth. The external field picture in the noon-midnight meridian plane resembles the picture formed by the magnetotail currents.

1. Introduction

The magnetospheric magnetic field is

$$\mathbf{B} = \mathbf{B}^{\text{int}} + \mathbf{B}^{\text{ext}} \tag{1}$$

where $\mathbf{B}^{\text{int}}$ is the field due to currents inside the Earth and $\mathbf{B}^{\text{ext}}$ is the field produced by magnetospheric currents. The internal field $\mathbf{B}^{\text{int}}$ is rather stable; the external field $\mathbf{B}^{\text{ext}}$ exhibits a strong variability. In particular, magnetic storms are accompanied by considerable variations in the magnetospheric magnetic field. The main characteristic of a magnetic storm is the hourly Dst index defined as the H component of the magnetic disturbance averaged over magnetograms of several low-latitude observatories located at different longitudes. The Dst index anticorrelates with the AE, AL, and Kp indexes which serve mainly to measure the substorm activity.

It is impossible to build a detailed distribution of the external magnetospheric field during a particular storm because of an insufficient number of spacecraft, and, therefore, we are limited to statistical studies. In previous works the external field was studied in relation with the other than Dst indexes or with the Dst index, but in separate limited magnetospheric regions. For instance, *Sugiura and Poros* [1973] considered the field at 3–23 R_E for quiet ($Kp = 0-1$) and slightly disturbed ($Kp = 2-3$) conditions. In the inner magnetosphere ($r < 5\ R_E$ at noon and $r < 10\ R_E$ at midnight) the external field was found to be directed preferentially in the negative z direction (in the SM coordinate system). A similar result was obtained by *Mead and Fairfield* [1975], who approximated the external field at the distances from 4 R_E to 17 R_E by second-degree polynomials in the geocentric distance.

The dependence of the field on the Dst index was analyzed in the equatorial plane at 2.3–3.6 R_E only. For these distances the empirical relation for the field averaged over longitude was obtained [*Sugiura*, 1973]

$$B_z^{\text{ext}} = -45 + 0.83\ Dst \tag{2}$$

The external field at 4–8.8 R_E near the equatorial plane was plotted by *Iijima et al.* [1990] for long disturbed periods ($2 \le Kp \le 6$, $-70 \le Dst \le -20$ nT). A strong azimuthal field inhomogeneity which is likely to be due to the fact that the current in the nightside magnetosphere is by a factor of 2 or 3 stronger than in the dayside magnetosphere was discovered.

Ostapenko and Maltsev [1997] approximated the fields at 3–10 R_E by the forth-degree polynomial in the geocentric distance. The polynomial coefficients were sought for as a linear combination of Dst and Kp indexes, dynamic solar wind pressure, and vertical IMF component. The dependence on Dst proved to be similar to that described by (2). With increasing distance from the Earth the dependence on Dst becomes weaker and at $r = 10\ R_E$ it is negligibly weak. Earlier a similar result was obtained by *Fairfield et al.* [1987]

Paper number GAI99314.
CCC: 1524–4423/2003/0303–0314$18.00

The online version of this paper was published 16 February 2003.
URL: http://ijga.agu.org/v03/gai99314/gai99314.htm
Print companion issued February 2003.

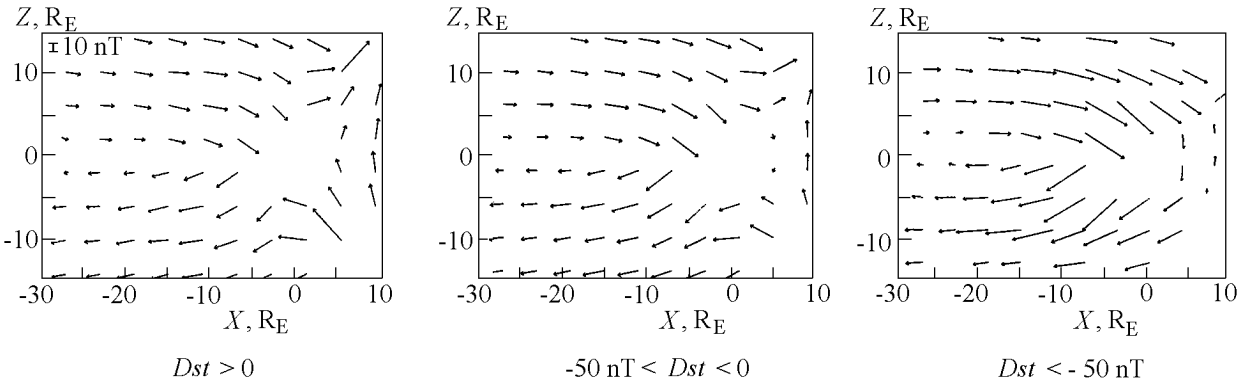

Figure 1. External magnetic field in the noon-midnight plane for three magnetic activity levels: (left) $Dst > 0$; (middle) $0 > Dst > -50$ nT; and (right) $Dst < -50$ nT.

for dependence of the external field on the Kp value.

So far the statistical dependence of the tail lobe field on the Dst index has not been studied. It was found that the tail lobe field grows with the AE index [*Baumjohann et al.,* 1990]; the AL index [*Nakai et al.,* 1991]; the southward IMF component [*Fairfield and Jones*, 1996; *Nakai et al.,* 1991]; and dynamic solar wind pressure [*Fairfield and Jones*, 1996; *Nakai et al.,* 1991; *Ostapenko and Maltsev,* 1998].

Up until now, the field variations caused by a storm have not been studied for the entire magnetosphere. The goal of this work was to investigate the response of the magnetic field at distances $-30R_E < x < 10R_E$; $-15R_E < y < 15R_E$; and $-15\,R_E < z < 15\,R_E$ to changes in the Dst index.

2. Treatment of the Data

The database described by *Fairfield et al.* [1994] was used. It includes more than 70,000 three-component magnetic field measurements carried out by 11 satellites in the region from 3 to 60 R_E during 20 years. All the magnetic field measurements are supplemented by hourly Dst indexes and 3-hour values of the Kp index. Sixty-seven percent of the data are complemented by hourly averages of the dynamic solar wind pressure p and three IMF components. For 47% of the data in the database, an hourly AE index is also given.

We used the data for the region $-30\,R_E < x < 10\,R_E$, $|y| < 15\,R_E$, and $|z| < 15\,R_E$. Depending on the Dst value, the initial data set was divided into three subsets. Table 1 shows the number of data points N in each subset and average values of Dst, Kp, AE, p, and IMF B_z. For each subset the external magnetic field was averaged over a three-dimensional mesh with the side length of 4 R_E.

In averaging, the dawn-dusk and north-south symmetries were taken into account. For distances $x > -10\,R_E$, the SM coordinate system with the z axis antiparallel to the Earth dipole axis was used. For distances $x < -10\,R_E$, in the magnetotail, the GSM coordinate system with the x axis pointed toward the Sun was employed. To improve spatial resolution in the vicinity of the neutral sheet which experiences considerable variations due to changes in the Earth dipole tilt, we introduced the coordinate $z = z_{\rm GSM} - z_{\rm ns}$, where $z_{\rm GSM}$ is the solar-magnetospheric coordinate and $z_{\rm ns}$ is the coordinate of the neutral sheet determined from the expression [*Peredo et al.,* 1993]

$$z_{\rm ns} = \left[(H_0 + D)\sqrt{1 - \frac{y^2}{y_0^2}} - D\right]\sin\psi \qquad |y| < y_0$$

$$z_{\rm ns} = -D\sin\psi \qquad |y| > y_0$$

where ψ is the Earth dipole tilt angle, $H_0 = 9\,R_E$, $D = 7\,R_E$, and $y_0 = 13.5\,R_E$.

3. Results

Figure 1 shows the magnetic field $\mathbf{B}^{\rm ext}$ due to external sources in the noon-midnight meridian plane for three magnetic activity levels: $Dst > 0$; $0 > Dst > -50$ nT; and $Dst < -50$ nT. In the tail lobes the field is nearly horizontal. It is evident that this field is produced by the electric

Table 1. Average Parameters for Three Subsets Differing by the Storm Activity Level

Conditions	Subset	N	Dst, nT	Kp	AE, nT	p, nPa	B_z IMF, nT
Quiet conditions	$Dst > 0$ nT	15,465	7	1.5	99	2.4	1.2
Weak storm	$0 > Dst > -50$ nT	47,952	−18	2.3	207	2.0	−0.1
Strong storm	$Dst < -50$ nT	4640	−74	4.3	445	3.4	−2.2

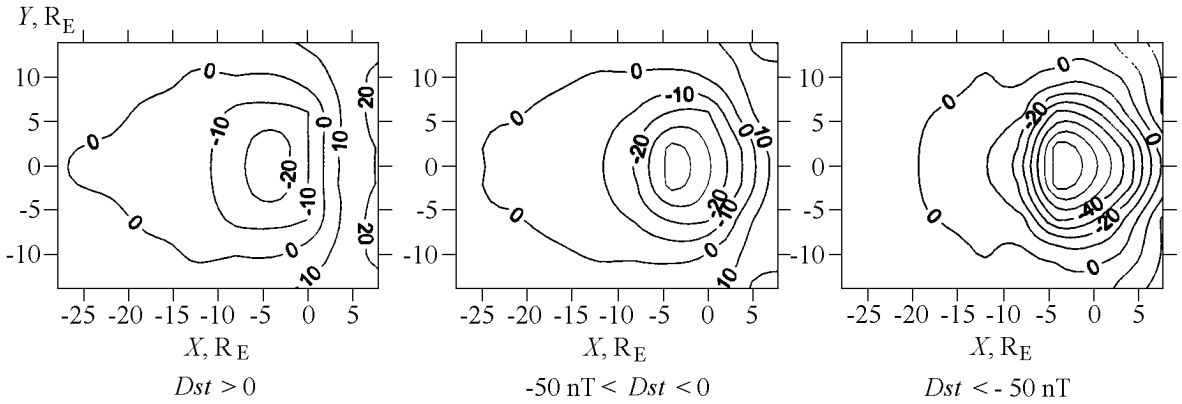

Figure 2. Isolines $B_z^{\rm ext}$ = const (in nT) in the equatorial plane.

current in the plasma sheet flowing from east to west. The current grows with increasing storm activity. On the front side of the magnetosphere (at $x > -10\,R_E$) the field has a more complicated structure.

Figure 2 shows isolines $B_z^{\rm ext}$ = const in the equatorial plane ($z = 0$). It can be seen that magnetic depression spreads over the major part of the magnetosphere. As the storm intensity grows, the depression deepens and expands.

Figures 3, 4, and 5 present isolines $B_x^{\rm ext}$ = const and $B_y^{\rm ext}$ = const in the $x = -20\,R_E$, $x = -10\,R_E$, and $x = 0$ planes, respectively. $B_x^{\rm ext}$ is seen to grow with increasing storm intensity. The $B_y^{\rm ext}$ component depends on the Dst index in the $x = -10\,R_E$ and $x = 0$ planes. The greatest increase in both components with storm enhancement is observed in the $x = 0$ plane.

To find the magnetospheric response to variations in the

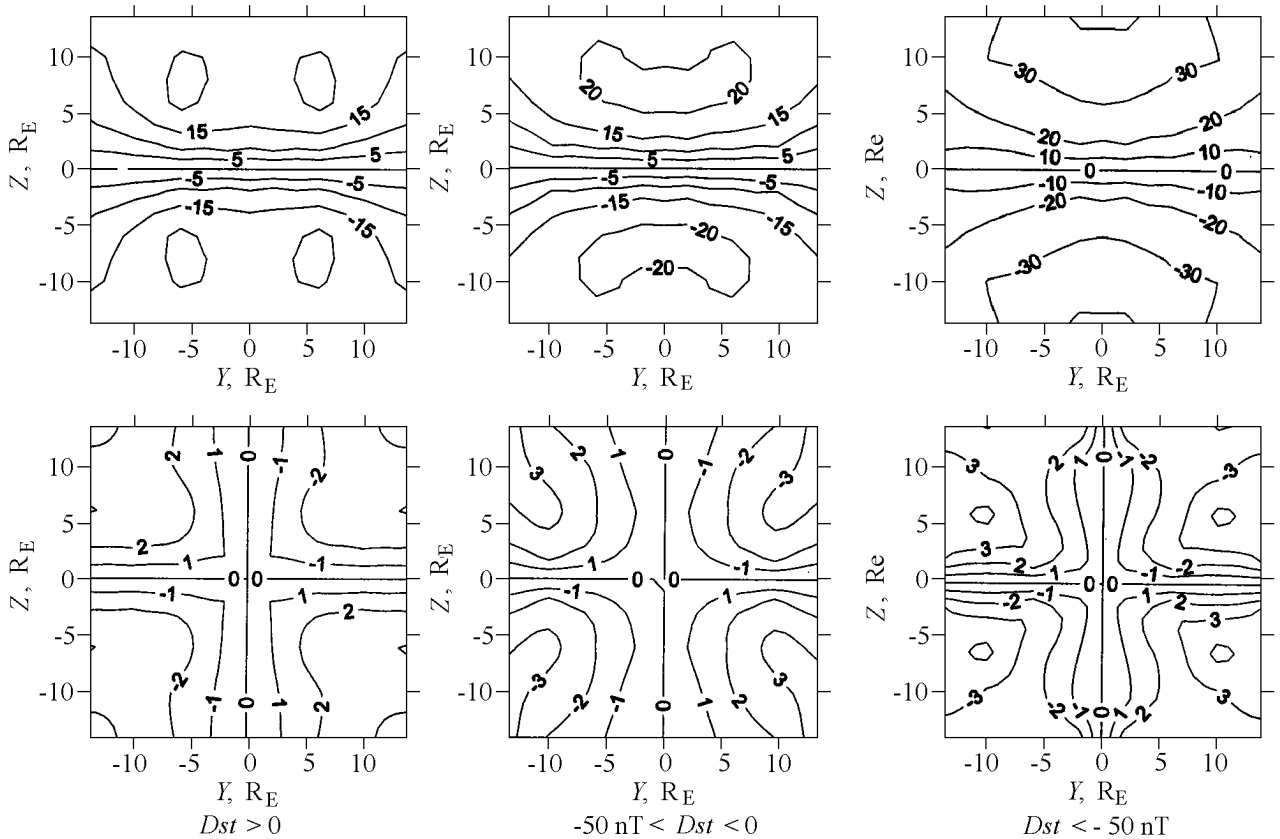

Figure 3. Isolines (top) $B_x^{\rm ext}$ = const and (bottom) $B_y^{\rm ext}$ = const in the plane $x = -20\,R_E$. The fields are expressed in nT.

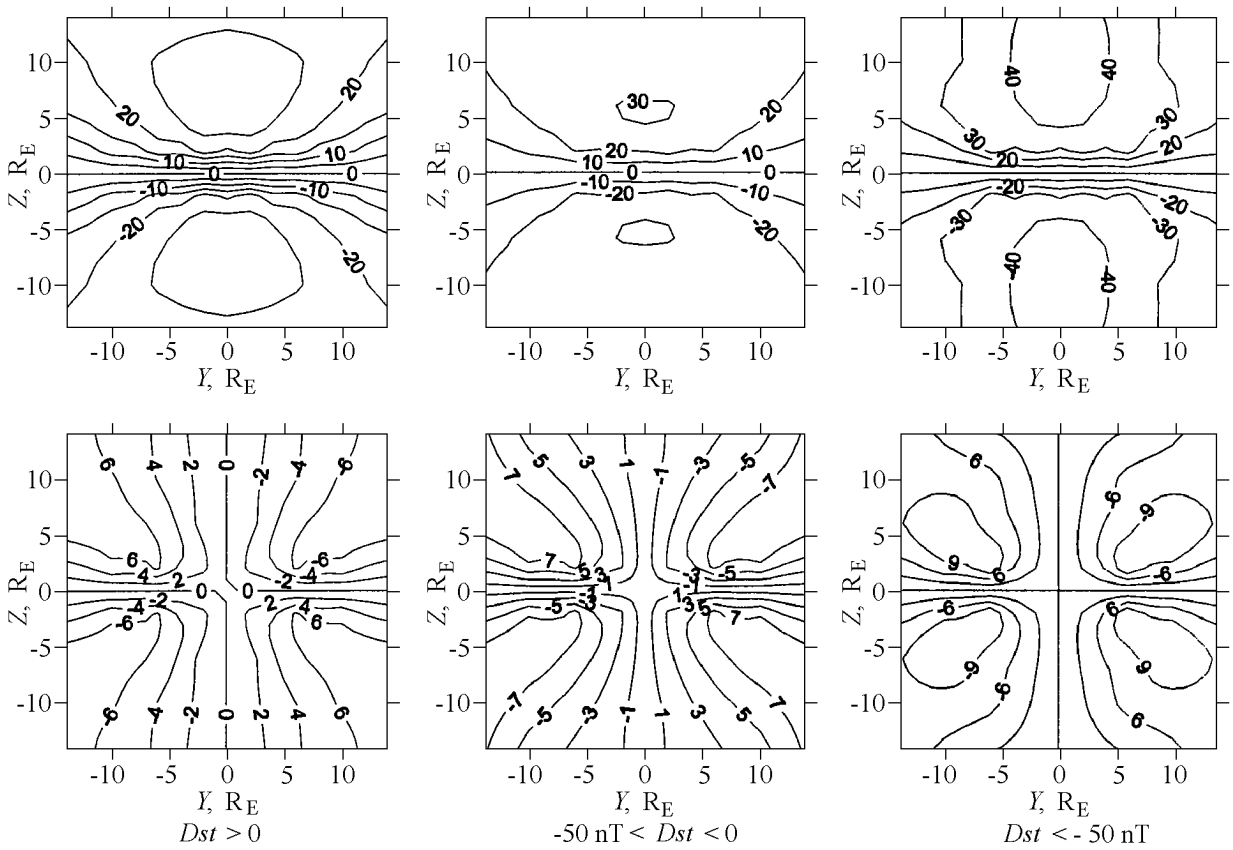

Figure 4. Same as Figure 3, but for the plane $x = -10\ R_E$.

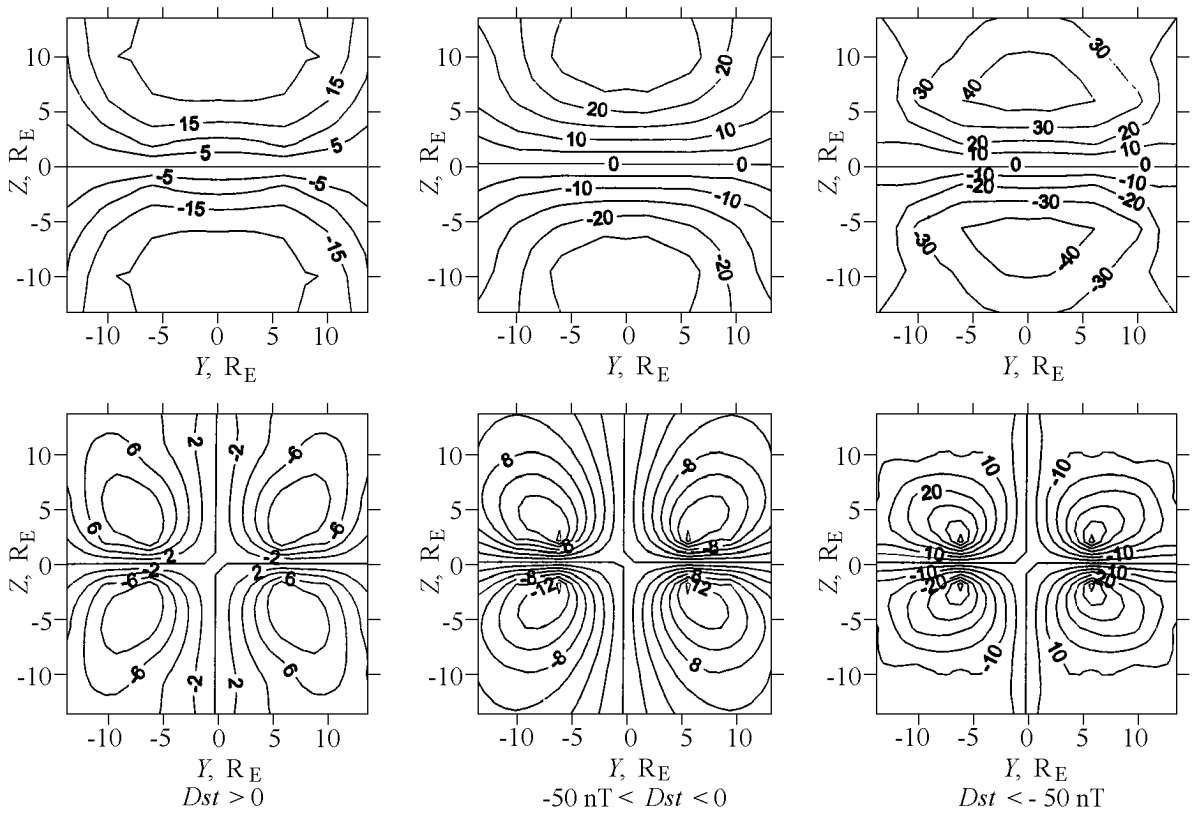

Figure 5. Same as Figure 3, but for the $x = 0$ plane.

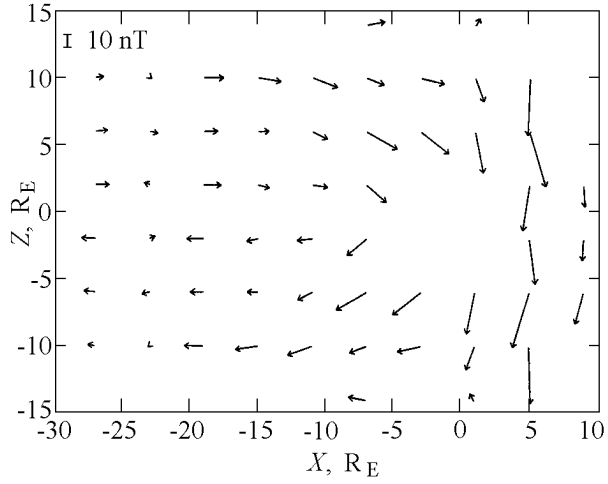

Figure 6. Difference between the storm time fields ($Dst < -50$ nT) and the fields in quiet conditions ($Dst > 0$) in the noon-midnight meridian plane.

Dst index, we subtracted Figure 1 (left) which corresponds to quiet conditions ($Dst > 0$), from Figure 1 (right) ($Dst < -50$ nT) plotted for the storm conditions. The result is shown in Figure 6.

4. Discussion

It is widely known that there exist five large-scale current systems in the magnetosphere: (1) the screening currents of the Earth dipole and the ring current at the magnetopause; (2) the symmetric ring current; (3) the current system consisting of the current across the magnetospheric tail and currents short-circuiting at the magnetopause; (4) the field-aligned currents of zone 1; (5) the field-aligned currents of zone 2 together with the partially-ring current. These five current systems are shown schematically in the left-hand side of Figure 7. Each current system is short-circuited. Thus, the external field $\mathbf{B}^{\text{ext}}$, is a sum of five magnetospheric currents:

$$\mathbf{B}^{\text{ext}} = \mathbf{B}_{\text{mp}} + \mathbf{B}_{\text{rc}} + \mathbf{B}_{\text{ct}} + \mathbf{B}_{\text{fa1}} + \mathbf{B}_{\text{fa2}} \qquad (3)$$

The fields of the currents at the magnetopause, ring current, tail current and field-aligned currents of zones 1 and 2 are in the right-hand side of formula (3), respectively. The fields of each of these currents in the noon–midnight meridian plane are schematically shown in the right-hand side of Figure 7.

Comparing Figure 1 to the right-hand side of Figure 7, one can see that the effect of the tail currents $\mathbf{B}_{\text{ct}}$ dominates at any level of magnetic activity. Only in the vicinity of the daytime magnetopause the field of the currents at the magnetopause $\mathbf{B}_{\text{mp}}$ prevails. The effect of the ring current $\mathbf{B}_{\text{rc}}$ is slightly pronounced. It is manifested evidently in the increase of the depression while approaching the Earth (Figure 2). The effect of the field-aligned currents $\mathbf{B}_{fa1}$ and $\mathbf{B}_{fa2}$ is manifested even weaker. Figures 3 and 4 show that the magnetic field in the tail lobes increases at the depression

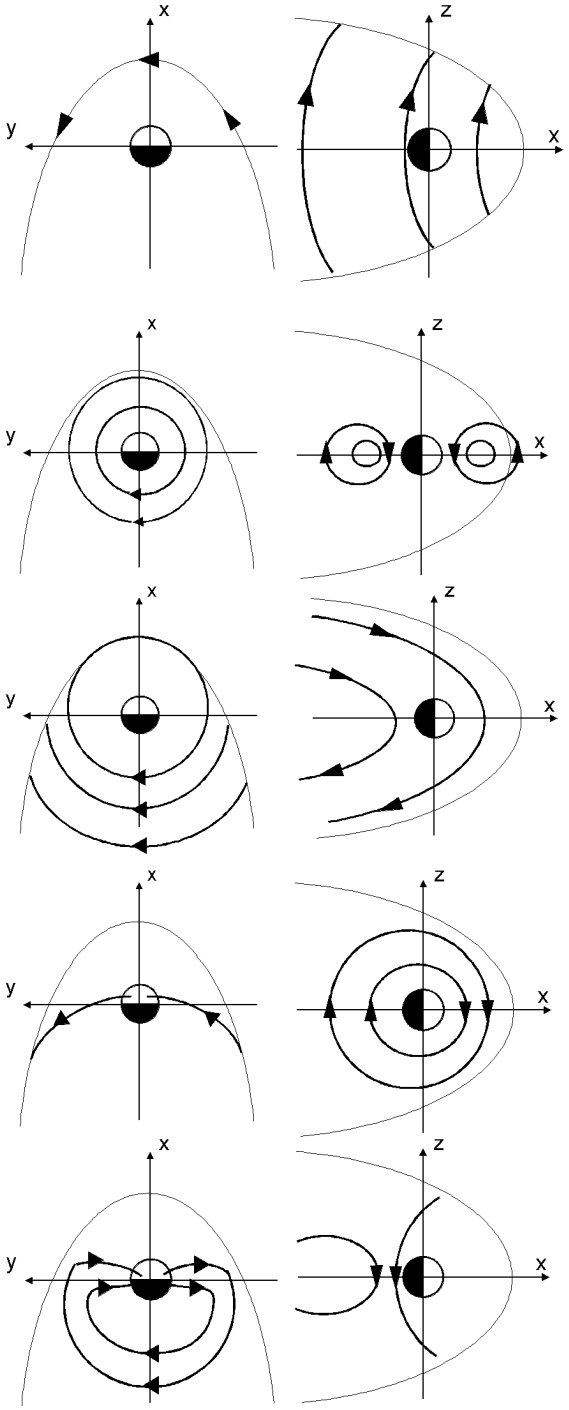

Figure 7. Electric currents (the left-hand side) and their magnetic fields (the right-hand side) for five elementary current systems. From top to bottom: the screening currents of the Earth dipole and the ring current at the magnetopause; the symmetric ring current; the current system consisting of the current across the magnetospheric tail and the short-circuiting currents at the magnetopause; the field-aligned currents of zone 1; the field-aligned currents of zone 2.

increase during a storm. It indicates to an intensification of the tail currents. Figure 5 shows that the most considerable increase of B_x during a storm occurs in the near-Earth part of the tail lobes at $x = 0$. This means that the closest part of the tail current is intensified. It is worth noting that according to Figure 7 the ring current gives $(\mathbf{B}_{\rm rc})_x = 0$ in the $x = 0$ plane. One may expect that the field-aligned currents of zone 1 (entering the ionosphere in the morning and leaving in the evening) are also intensified during a storm. The x component of the field of the field-aligned and tail currents is of the same sign above the Earth poles (see Figure 7). At the magnetic shells located deeper than the field-aligned current the B_x component induced by the field-aligned current changes its sign, thus reducing the field in the low-latitude parts of the nearest tail lobe. Thus, the field-aligned current leads to a irregularity of the magnetic field in the nearest lobe. This irregularity is seen in the top part of Figure 5. However it is not well pronounced and this means that the tail currents produce stronger effect in the $x = 0$ plane than the field-aligned currents. The field-aligned currents of zone 2 short-circuited to the partially-ring current should also be intensified during a storm. The magnetic field of the given current system is in a way similar to the fields formed by the tail and ring currents. Usually it is accepted that the total field-aligned current of zone 2 is about 70% of the zone 1 currents. Since no effects of the zone 1 currents are seen in Figures 1–5, the zone 2 field-aligned currents hardly impact considerably on the field distribution in the magnetosphere. The B_y component of the external field almost does not depend on Dst at the distance $x = -20\,R_E$ (Figure 3). A weak dependence on Dst appears at the distance $x = -10\,R_E$ (Figure 4). In the $x = 0$ plane passing though the center of the Earth, the dependence of the B_y component on the storm intensity is very strong (Figure 5). The magnetic depression occurs in the major part of the magnetospheric equatorial plane at all activity levels (see Figure 2). With an increase of the storm activity the depression becomes deeper and covers more distant regions. The epicenter of the depression is shifted relative to the Earth center by about $3\,R_E$ towards the nightside. It should be noted that there is no measurements at the distances less than $3R_E$ so the isolines in this region in Figure 2 are a result of an interpolation. *Sugiura* [1973] studied the field in the equatorial plane at distances of $2.3-3.6\,R_E$. For the field averaged over longitudes the empirical relation (2) was obtained. *Iijima et al.* [1990] drew a distribution of the field in the vicinity of the equatorial plane at distances of $4 - 8.8R_E$ for the $-70 \le Dst \le -20$ nT conditions at the mean value $Dst = -34$ nT. The field distribution in Figure 2 resembles the field obtained in the above-mentioned publications but differs by better smoothness. Apparently it is due to the fact that we have averaged the field within larger sells. Otherwise there would not be enough data to derive the field dependence on the Dst index in the entire volume of the magnetosphere. The differential field shown in Figure 6 most of all resembles the $\mathbf{B}_{\rm ct}$ field in Figure 7. This means that at the storm intensification mainly the tail current is increased.

5. Conclusions

Variations in the external magnetic field at distances up to 30 R_E have been studied as a function of storm intensity. It has been shown that for all storm activity levels the effect of magnetotail currents dominates. As the storm enhances, the tail current effect becomes stronger. The field due to magnetopause currents prevails in the distant region of the dayside magnetosphere.

Acknowledgment. The work was supported by Russian Foundation for Basic Research (project 99-05-64557).

References

Baumjohann, W., G. Paschmann, and H. Luhr, Pressure balance between lobe and plasma sheet, *Geophys. Res. Lett., 17*, 45, 1990.

Fairfield, D. H., and J. Jones, Variability of the tail lobe field strength, *J. Geophys. Res., 101*, 7785, 1996.

Fairfield, D. H., M. H. Acuna, L. J. Zanetti, and T. A. Potemra, The magnetic field of the equatorial magnetotail: AMPTE/CCE observations at $R < 8.8\,R_E$, *J. Geophys. Res., 92*, 7432, 1987.

Fairfield, D. H., N. A. Tsyganenko, A. V. Usmanov, and M. V. Malkov, A large magnetosphere magnetic field database, *J. Geophys. Res., 99*, 11,319, 1994.

Iijima, T., T. A. Potemra, and L. J. Zanetti, Large-scale characteristics of magnetospheric equatorial currents, *J. Geophys. Res., 95*, 991, 1990.

Mead, G. D., and D. H. Fairfield, A quantitive magnetospheric model derived from spacecraft magnetometer data, *J. Geophys. Res., 80,* 523, 1975.

Nakai, H., Y. Kamide, and C. T. Russell, Influences of solar wind parameters and geomagnetic activity on the tail lobe magnetic field: A statistical study, *J. Geophys. Res., 96*, 5511, 1991.

Ostapenko, A. A., and Yu. P. Maltsev, Relation of the magnetic field in the magnetosphere to the geomagnetic and solar wind activity, *J. Geophys. Res., 102*, 17,467, 1997.

Ostapenko, A. A., and Yu. P. Maltsev, Three-dimensional magnetospheric response to variations in the solar wind dynamic pressure, *Geophys. Res. Lett., 25*, 261, 1998.

Peredo, M., D. P. Stern, and N. A. Tsyganenko, Are existing magnetospheric models excessively stretched?, *J. Geophys. Res., 98,* 15,343, 1993.

Sugiura, M., Quiet time magnetospheric field depression at 2.3–3.6 R_E, *J. Geophys. Res., 78,* 3182, 1973.

Sugiura, M., and D. J. Poros, A magnetospheric field incorporating the Ogo 3 and 5 magnetic field observations, *Planet. Space Sci., 21*, 1763, 1973.

Yu. P. Maltsev and A. A. Ostapenko, Polar Geophysical Institute, Apatity, Murmansk Region, Russia.
(maltsev@pgi.colasc.net.ru)

(Received 5 June 1999; revised 13 December 2002;
accepted 10 February 2003)